

Standard Model Higgs Boson Searches at the Tevatron

Kyle J. Knoepfel^{1,2}

(*On behalf of the CDF and D0 collaboration*)

Fermi National Accelerator Laboratory

Abstract

Updated Standard Model Higgs boson search results from the Tevatron experiments are presented. We focus on the updated CDF $\cancel{E}_T + b\bar{b}$ result, where a significant shift in observed limits is explained. For the Tevatron combinations, upper limits at 95% credibility level and best-fit values for the Higgs boson cross section times branching ratio are presented. We also place constraints on the Higgs couplings to fermions and electroweak vector bosons. All results are consistent with the existence of a Standard Model Higgs boson with a mass of $125 \text{ GeV}/c^2$, and with the Standard-Model predictions associated with that assumption.

1 Introduction

In the context of the Standard Model (SM) of particle physics [1], the Higgs mechanism [2] has been postulated to instigate electroweak symmetry breaking, which produces the electroweak W^\pm and Z bosons. The mechanism gives rise to a new scalar particle, the Higgs boson, which has been the object of many experimental searches for the past few decades.

In July 2012, the ATLAS and CMS experiments separately claimed discovery of a particle with a mass of $125 \text{ GeV}/c^2$ that is consistent with a SM Higgs boson interpretation [3]. To identify the new state as the SM Higgs boson, however, requires that measurements of its couplings to fermions and electroweak bosons, as well as measurements of its production cross-sections and decay branching fractions are consistent with SM predictions. To this end, the Tevatron experiments in August 2012 jointly claimed evidence of a new particle that decayed to a $b\bar{b}$ pair that was consistent with the LHC discoveries and the SM predictions [4].

¹E-mail: knoepfel@fnal.gov

²Contributed to the Proceedings of Les Rencontres de Physique de la Vallée d'Aoste, March 2013, La Thuile, Italy.

Whereas the primary sensitivities of the 125-GeV/ c^2 particle at the LHC are due to the relatively clean gluon-fusion $H \rightarrow \gamma\gamma$ and $H \rightarrow Z^{(*)}Z$ modes, where both Z bosons (one produced on shell) decay to pairs of leptons, the cross sections of such modes at the Tevatron are largely suppressed due to the lower center-of-mass energy. The primary sensitivities in Higgs boson searches at the Tevatron, therefore, come mainly from the associated production modes (VH), where the Higgs boson is produced alongside an electroweak boson V (which represents the W or Z), and the Higgs boson decays via $H \rightarrow b\bar{b}$.

As the b -quarks are often produced at energies greater than 50 GeV in the laboratory reference frame, they fragment into a cascade of less energetic particles, which eventually hadronize at the scale of Λ_{QCD} . Various reconstruction algorithms are optimized to collect as much energy of these “jets” (and therefore the original b quark) as possible, without introducing extra energy from same-event particles that are unassociated with the original b -quark. Although each experiment applies jet-energy corrections which adjust the jet energies back to the quark-level quantities, the rms of these corrections tends to be on the order of 10-20% of the overall scale. If a Higgs boson that decays via $H \rightarrow b\bar{b}$ exists, the dijet invariant mass of the system is thus not able to constrain well the mass of the Higgs boson, unlike the $H \rightarrow \gamma\gamma$ and $H \rightarrow Z^{(*)}Z$ searches. Rather, the overall production rate, and other quantities must be used to place constraints on the allowed Higgs boson mass at the Tevatron experiments in this channel.

In this contribution, we discuss the current status of the individual Tevatron Higgs searches (up to March 2013), as well as the Tevatron combinations at CDF, D0, and the combined results from both experiments. For the combinations, in addition to excluding the Higgs boson across a putative mass range of $100 < m_H < 200$ GeV/ c^2 , we also present best-fit values of the cross-section times branching ratio, and place constraints on the HVV and Hff couplings. We do not discuss fermiophobic or fourth-generation searches, which are presented in an upcoming publication [5].

2 Status of the Individual Tevatron Searches

The CDF and D0 experiments have many analyses in the final stages of presentation. Table 1 presents the *current* publication status of the Tevatron experiments that went into the presentation at the La Thuile conference in March 2013³. Of the searches presented in Table 1, we will focus on the CDF $\cancel{E}_T + b\bar{b}$ Higgs search result as it is the analysis with the most significant updates since the last conference (HCP 2012 in Kyoto, Japan).

³To avoid confusion in citing publications, we present the publication status of each individual search current as of submission of this proceedings contribution, and not the status at the time of the conference presentation.

Table 1: Status of Tevatron Higgs boson searches – new since the HCP 2012 conference.

Experiment	Search	Status
CDF	$VH \rightarrow \cancel{E}_T + b\bar{b}$	Published in Phys. Rev. D [6]
	$VH \rightarrow q\bar{q}' + b\bar{b}$	Published in J. High Energy Physics [7]
D0	$\ell\nu$ +jets searches	Accepted by Phys. Rev. D [8]
	$H \rightarrow W^+W^-$	Accepted by Phys. Rev. D [9]
	$H \rightarrow \gamma\gamma$	Accepted by Phys. Rev. D [10]
	$H \rightarrow W^+W^-/\tau^+\tau^-$	Accepted by Phys. Rev. D [11]
	Trilepton/same-sign $e\mu$ pairs	Accepted by Phys. Rev. D [12]

2.1 $\cancel{E}_T + b\bar{b}$ Higgs Search at CDF

The $VH \rightarrow \cancel{E}_T + b\bar{b}$ Higgs search [6] is sensitive to the $ZH \rightarrow \nu\bar{\nu} + b\bar{b}$ and $WH \rightarrow \ell\nu + b\bar{b}$ processes, which contain intrinsic missing transverse energy (\cancel{E}_T). In the first case, the \cancel{E}_T results from the undetectable $\nu\bar{\nu}$ pair, whereas for the second case, the \cancel{E}_T is from the undetectable neutrino and an identified charged lepton ℓ . For this search, events with one identified charged lepton are vetoed, ensuring orthogonality of data samples with respect to the CDF $WH \rightarrow \ell\nu + b\bar{b}$ search. A minimum \cancel{E}_T requirement of 35 GeV is made of the event to reduce background from events with two or more reconstructed jets produced by QCD (“QCD multijet”), but where a significant energy imbalance occurs from jet-energy miscalculation. Despite this requirement, QCD multijet backgrounds remain dominant, and multivariate algorithms are implemented to further separate the QCD background (and other SM backgrounds) from the Higgs boson signal. To increase the signal-to-background ratios, the analysis is split into tagging categories based on the probability that the jets originated from b -quarks.

To improve sensitivity to Higgs boson exclusion relative to the previous analysis [14], an updated b -tagging algorithm was implemented, which was specifically optimized for $H \rightarrow b\bar{b}$ searches [13]. Due to correlations between the new tagging algorithm and the background modeling procedure, new QCD background shape models and QCD-suppression multivariate algorithms needed to be derived and retrained, respectively. Figure 1 shows the 95% credibility level (C.L.) limits for the previous analysis and the updated analysis. Even though the only dominant change in analysis methodology is the implementation of an improved b -tagging algorithm in the newer analysis, a fairly significant shift in the observed limits is seen (55% on average), whereas a 14% improvement is expected.

A non-negligible portion of the shift in observed limits is due to a different treatment of systematic uncertainties between b -tag categories. However, the primary reason for the remaining change in the shift is due to significant event migration between the b -tagging categories of the previous analysis, and those of the updated one. A two-sided p -value was calculated to estimate that the remaining shift in observed limits between both analyses was due to statistical effects of event migration. Accounting for the statistical correlations between the two analyses, and the correlations between each

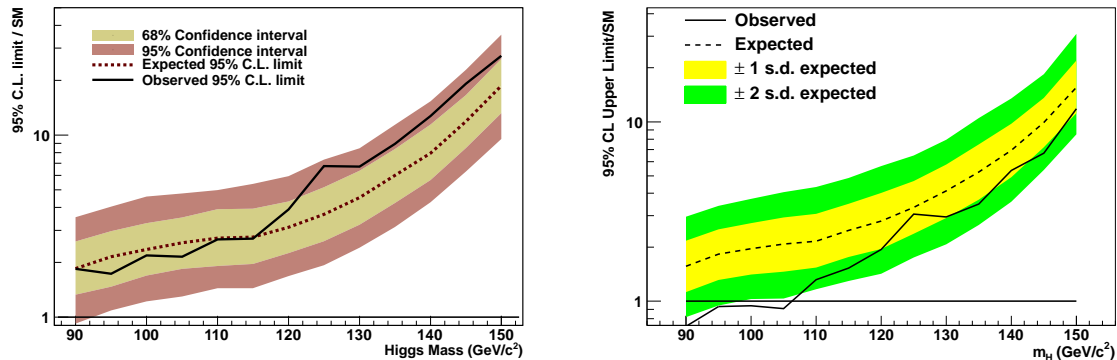


Figure 1: Upper limits (95% C.L.) on Higgs boson production in the $\cancel{E}_T + b\bar{b}$ channel for the (left) previous analysis [14] and (right) the updated analysis [6].

m_H hypothesis, the probability that the non-systematic change in observed limits is due to statistical effects only is at the 3%-5% level. As no background mismodeling was observed in the updated analysis, and as applying the updated treatment of systematic uncertainties to the previous analysis did not significantly alter any of the previous results, we conclude that the significant shift in observed limits is due primarily to statistical effects of event migration. For further details, see Ref. [6].

2.2 CDF Combination Considerations

Even though the previous and updated versions of the CDF $\cancel{E}_T + b\bar{b}$ analysis use different b -tagging techniques, both analyses are robust in terms of background modeling, and in accounting for systematic effects. Both results are therefore interpreted as correct, but different ways of analyzing the same Higgs boson search channel. For the final combination, however, CDF uses the analysis that gives the best sensitivity to excluding the Higgs at 95% C.L.—thus, the updated $\cancel{E}_T + b\bar{b}$ result was used in the final CDF and Tevatron Higgs boson combinations.

3 Status of the Tevatron Combinations

At the time of the conference, the final CDF Higgs boson combination had been submitted for publication and was thus available for public presentation [15]. The final D0 and Tevatron combinations were not yet public, so combinations from October 2012 and November 2012, respectively, were presented and are also shown here.

3.1 Upper Limits and Best-fit Values on Higgs Production

The individual 95% C.L. upper limits on the Higgs production cross section times branching ratio are shown in fig. 2 in units of the SM prediction. Excesses in the

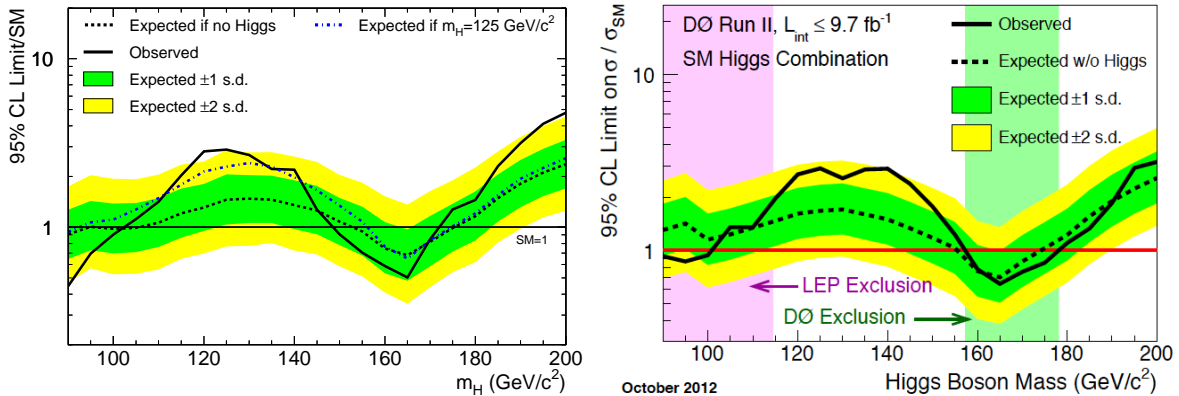


Figure 2: Upper limits (95% C.L.) on Higgs production $\sigma \times \mathcal{B}$ for (left) CDF and for (right) D0 in units of the SM prediction.

observed limits are seen in both experiments in the range $100 \lesssim m_H \lesssim 150 \text{ GeV}/c^2$. Higgs boson mass regions are excluded where the observed line falls below unity. The CDF plot also shows what one would expect to see if there were a 125-GeV/ c^2 Higgs boson present in the data.

The CDF-D0 combined (Tevatron) upper limits and best-fit production rates are shown in fig. 3, where correlated uncertainties between both experiments have been taken into account. Both plots show the expected shape of the data if a 125-GeV/ c^2 Higgs boson were present in the data, produced at 50% greater rate than is predicted in the SM. The right plots also shows the best-fit value for the Higgs boson production produced at the nominal SM prediction. As can be seen, the Tevatron data prefer a scenario that assumes the presence of a Higgs boson instead of the non-Higgs boson hypothesis (black, dashed line). One can take a slice of the right plot in fig. 3 for $m_H = 125 \text{ GeV}/c^2$ and decompose the best-fit $\sigma/\sigma_{\text{SM}}$ into the individual search channels. This is shown in fig. 4. The combined and individual-channel best-fit results are consistent with the SM predictions to within one standard deviation, with the exception of the $H \rightarrow \gamma\gamma$ search, which exceeds it by roughly 1.5 standard deviations.

3.2 Constraints on Higgs Couplings

In addition to deriving limits and extracting best-fit values on the Higgs boson cross section times branching ratio, the Tevatron experiments also place constraints on the Higgs couplings to fermions and the electroweak vector bosons. This is done by introducing coefficients κ_i that scale the $H\bar{i}i$ SM couplings, where $i = f$ (fermions), $i = Z$, $i = W^\pm$, or $i = V$ when no distinction is made between the electroweak vector bosons. The SM couplings are obtained when $\kappa_i = 1$. At the Tevatron, the most sensitive-to-exclusion search channels have $\sigma \times \mathcal{B}$ expressions that are mostly proportional to the product $\kappa_f \kappa_V$. However, the $\sigma \times \mathcal{B}$ expressions of the less sensitive channels $t\bar{t}H \rightarrow t\bar{t} + b\bar{b}$ and $VH \rightarrow V + W^+W^-$ are proportional to κ_f^2 and κ_V^2 , respectively.

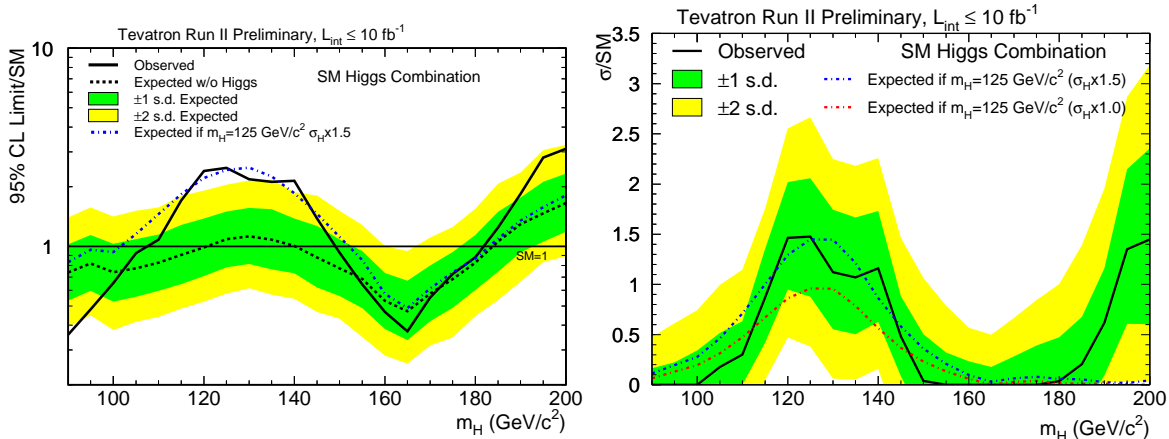


Figure 3: Tevatron combination for the (left) 95% C.L. upper limits on the Higgs production rate and for the (right) best-fit value of the $\sigma \times \mathcal{B}$ as determined from the data. Both plots are presented in units of the SM prediction.

Search channels that do not dominate the exclusion sensitivity can therefore provide sensitivity to constraining the Higgs couplings.

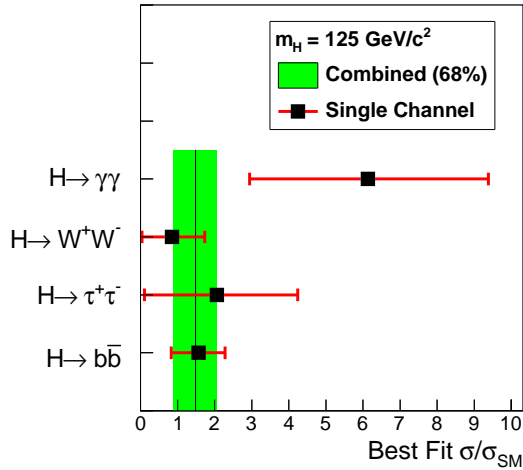
Figure 5 shows two-dimensional posterior probability densities for constraining κ_f vs. κ_V , and κ_Z vs. κ_W . Due to an interference term in the $H \rightarrow \gamma\gamma$ $\sigma \times \mathcal{B}$ expression, the excess in the $H \rightarrow \gamma\gamma$ search leads to a slight preference for solutions in the second and fourth quadrants in the left plot of the fig. 5. The SM prediction, however, is consistent with the Tevatron data just outside of one standard deviation. The right plot of fig. 5 tests for custodial symmetry, which in the SM guarantees $\kappa_Z = \kappa_W = 1$. The Tevatron data are consistent with this prediction to well within one standard deviation.

4 Conclusions

Whereas the results of the individual search channels have not changed greatly since November 2012, the updated CDF $\cancel{E}_T + b\bar{b}$ analysis [6] has extensively studied the change in observed limits since the publication of the previous result [14]. The large change in observed limits is due to statistical effects of event migration by switching to an improved b -tagging algorithm.

We have presented Tevatron combinations of upper limits (95% C.L.) and best-fit values of the Higgs boson cross section times branching ratio. We see an excess in data that is consistent with a 125-GeV/ c^2 Higgs boson interpretation. In addition, we place constraints on the Higgs couplings to fermions and electroweak vector bosons, the results of which are largely consistent with SM predictions.

Tevatron Run II Preliminary, $L \leq 10 \text{ fb}^{-1}$



Preliminary Results (Nov. 2012)	
Process	Best-fit $\sigma \times \mathcal{B}/\text{SM}$
$H \rightarrow W^+W^-$	$0.88^{+0.88}_{-0.81}$
$H \rightarrow b\bar{b}$	$1.56^{+0.72}_{-0.73}$
$H \rightarrow \gamma\gamma$	$6.13^{+3.25}_{-3.19}$
$H \rightarrow \tau^+\tau^-$	$2.12^{+2.25}_{-2.12}$
Combined	$1.48^{+0.58}_{-0.60}$

Figure 4: Best-fit values for Higgs boson cross section and times branching ratio for individual search channels, as well as for the combined result. The table at the right is the numerical form of the plot on the left.

Addendum

Since the conference, additional analyses have been submitted and accepted for publication from the D0 collaboration: the above-mentioned full Tevatron combination [5], the $ZH \rightarrow \ell\ell + b\bar{b}$ search [16] and the full D0 combination [17].

Acknowledgments

The author would like to thank the organizers for an enjoyable experience at the Les Rencontres de Physique de la Vallée d’Aoste conference, and the support of Fermilab and the CDF experiment.

References

- [1] S. Glashow, Nucl. Phys. **22**, 579 (1961); S. Weinberg, Phys. Rev. Lett. **19**, 19 (1967); A. Salam, *Elementary Particle Theory*, edited by Almqvist and Wiksell (Stockholm, Sweden) p. 367 (1968).
- [2] F. Englert F. and R. Brout, Phys. Rev. Lett. **13**, 321 (1964); P.W. Higgs, Phys. Rev. Lett. **13**, 508 (1964); G.S. Guralnik, C.R. Hagen, and T.W.B. Kibble, Phys. Rev. Lett. **13**, 585 (1964).
- [3] S. Chatrchyan *et al* (CMS Collaboration), Phys. Lett. B **716**, 30 (2012); G. Aad *et al* (ATLAS Collaboration), Phys. Lett. B **716**, 1 (2012).

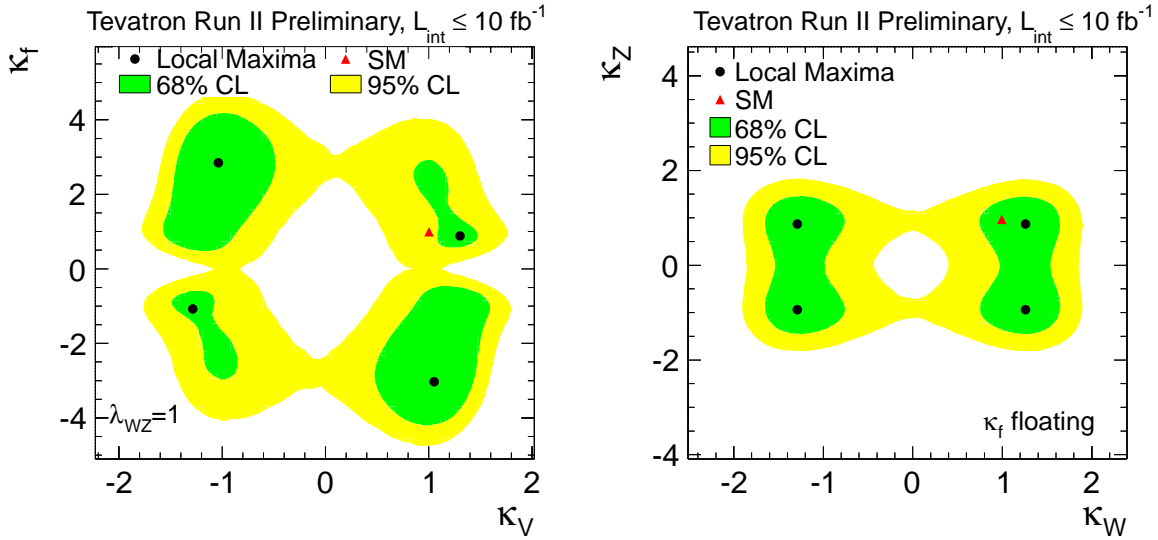


Figure 5: Two-dimensional posterior probability densities for constraining (left) κ_f vs. κ_V , and (right) κ_Z vs. κ_W . For the left plot κ_W/κ_Z is assumed to be unity, whereas for the right plot, κ_f is allowed to vary.

- [4] T. Aaltonen *et al* (CDF and D0 Collaborations), Phys. Rev. Lett. **109**, 071804 (2012).
- [5] T. Aaltonen *et al* (CDF and D0 Collaborations), Accepted by Phys. Rev. D, arXiv:1303.6346 [hep-ex].
- [6] T. Aaltonen *et al* (CDF Collaboration), Phys. Rev. D **87**, 052008 (2013).
- [7] T. Aaltonen *et al* (CDF Collaboration), J. High Energy Phys. 02, 004 (2013).
- [8] V.M. Abazov *et al* (D0 Collaboration), Accepted by Phys. Rev. D, arXiv:1301.6122 [hep-ex].
- [9] V.M. Abazov *et al* (D0 Collaboration), Accepted by Phys. Rev. D, arXiv:1301.1243 [hep-ex].
- [10] V.M. Abazov *et al* (D0 Collaboration), Accepted by Phys. Rev. D, arXiv:1301.5358 [hep-ex].
- [11] V.M. Abazov *et al* (D0 Collaboration), Accepted by Phys. Rev. D, arXiv:1211.6993 [hep-ex].
- [12] V.M. Abazov *et al* (D0 Collaboration), Accepted by Phys. Rev. D, arXiv:1302.5723 [hep-ex].
- [13] J. Freeman *et al*, Nucl. Instrum. Methods Phys. Res., Sect. A **697**, 64 (2013).

- [14] T. Aaltonen *et al* (CDF Collaboration), Phys. Rev. Lett. **109**, 111805 (2012).
- [15] T. Aaltonen *et al* (CDF Collaboration), Accepted by Phys. Rev. D, arXiv:1301.6668 [hep-ex].
- [16] V.M. Abazov *et al* (D0 Collaboration), Accepted by Phys. Rev. D, arXiv:1303.3276 [hep-ex].
- [17] V.M. Abazov *et al* (D0 Collaboration), Accepted by Phys. Rev. D, arXiv:1303.6346 [hep-ex].